Zero-Phase Filtering for Lightning Impulse Evaluation: A K-factor Filter for the Revision of IEC60060-1 and -2

Paul L. Lewin, *Member, IEEE*, Trung N. Tran, David J. Swaffield, *Member, IEEE*, and Jari K. Hällström

***Abstract*—The next revision of the international standard for high-voltage measurement techniques, IEC 60060-1, has been planned to include a new method for evaluating the parameters associated with lightning impulse voltages. This would be a significant improvement on the loosely defined existing method which is, in part, reliant on operator judgment and would ensure that a single approach is adopted worldwide to determine peak voltage, front, and tail times, realizing standardization in measured parameters across all laboratories. Central to the proposed method is the use of a K-factor to attenuate oscillations and overshoots that can occur with practical generation of impulse voltages for testing on high-voltage equipment. It is proposed that a digital filter that matches the K-factor gain characteristic be implemented and used for this purpose. To date, causal filter designs have been implemented and assessed. This paper is concerned with the potential application of a noncausal digital filter design to emulate the K-factor. The approach has several advantages; the resulting design is only second order, it can be designed without using optimization algorithms, it is a zero-phase design and it matches the K-factor almost perfectly. Parameter estimation using waveforms from the IEC 61083-2 test data generator and experimental impulse voltages has been undertaken and obtained results show that the zero-phase filter is the ideal digital representation of the proposed K-factor. The effect of evaluating parameters by the proposed method is compared to mean-curve fitting and the challenge of effective front-time evaluation is discussed.**

***Index Terms*—Digital filters, high-voltage techniques, IEC 60060-1, impulse testing, pulse measurements, zero-phase filter.**

I. Introduction

IEC 60060-1 and -2 are established international standards that cover requirements for high-voltage testing techniques and related measurement systems. The scopes of these standards include specification of the equipment and methods for measurement of the standard lightning impulse voltages that are used to test power equipment. A typical impulse voltage waveform is shown in Fig. 1; this waveform is generally described using three parameters, namely, the peak voltage $\mathrm{U_P}$, the front time, $\mathrm{T_1}$, and the tail time $\mathrm{T_2}$. Referring to Fig. 1, the standard method for determining the front time from an experimental measurement is to measure the time for the impulse voltage waveform to increase from 30% to 90% of its peak value, this time is then scaled to represent the total front time, i.e.,

$$\mathrm{T_1} = 1.67(\mathrm{t_{90}} - \mathrm{t_{30}}) \quad 0.84\,\mu\mathrm{s} \le \mathrm{T_1} \le 1.56\,\mu\mathrm{s}. \tag{1}$$

The IEC 60060-1 [1] specification requires that for the waveform to be acceptable for testing purposes, the front time must be within $\pm 30\%$ of the nominal 1.2-μs front time. The tail time requires the definition of the origin $(\mathrm{t_0})$ of the impulse waveform. The origin can be found using the 30% and 90% voltages and times, i.e.,

$$\mathrm{t_0} = \mathrm{t_{30}} - \frac{\mathrm{U_{30}}}{\mathrm{U_{90}} - \mathrm{U_{30}}}(\mathrm{t_{90}} - \mathrm{t_{30}}). \tag{2}$$

The tail time is equated as the time difference between the time taken for the waveform to decay to 50% of the peak voltage and $\mathrm{t_0}$, i.e.,

$$\mathrm{T_2} = \mathrm{t_{50}} - \mathrm{t_0} \quad 40\,\mu\mathrm{s} \le \mathrm{T_2} \le 60\,\mu\mathrm{s}. \tag{3}$$

In this case, the standard defines an acceptable waveform as one whose tail time is within $\pm 20\%$ of the nominal 50-μs value.

The peak voltage is acceptable if it is within 3% of the desired peak value, assuming that an approved measuring system is used. It is accepted that some test circuits may have oscillations or an overshoot at the peak of the impulse.

The current version of IEC 60060-1 requires that if the frequency of any oscillation is greater than 500 kHz or the duration of the overshoot is less than 1 μs, then the peak voltage can be determined from a mean curve. Oscillations or overshoot close to the peak of the impulse are deemed acceptable provided that their peak amplitude is less than 5% of the peak voltage. This definition is not particularly practical and is open to interpretation. The application of digital filters to remove oscillation and overshoot primarily to assist in the calibration of

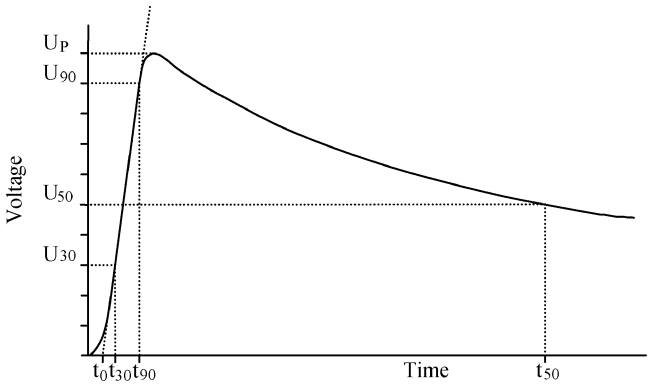

Fig. 1. Definitions for the calculation of lightning impulse voltage waveform parameters.

Manuscript received June 14, 2006; revised December 6, 2006. Paper no. TPWRD-00333-2006.

P. L. Lewin, T. N. Tran, and D. J. Swaffield are with the Tony Davies High Voltage Laboratory, School of Electronics and Computer Science, University of Southampton, Southampton SO17 1BJ, U.K. (e-mail: pll@ecs.soton.ac.uk).

J. K. Hällström is with TKK, Espoo, Finland (e-mail: jari.hallstrom@tkk.fi).

Digital Object Identifier 10.1109/TPWRD.2007.911124

impulse voltage measurement systems has been reported [2] and more recently, interest is growing in the use of digital techniques to automatically determine experimentally measured impulse waveform parameters [3]. The adoption of such methods will benefit standardization, ensuring that all laboratories use identical techniques for parameter evaluation.

Therefore, a new method for evaluating the lightning impulse parameters will be proposed in the next revision of IEC 60060-1, based on a study of the response of different insulation materials to oscillations on smooth lightning impulses. The K-factor has been determined as a result of comprehensive tests conducted at several European laboratories [4]. This project was funded by the standards, measurement, and testing (SMT) program of the European Commission, and it was performed in coordination with CIGRE Working Group D1.33.

The intention is that the application of this smoothing function will attenuate oscillations and overshoots, thus ensuring consistent parameter evaluation. The K-factor characteristic has been defined as

$$\mathrm{K_T} = \frac{1}{1+\mathrm{af}^2} \quad \mathrm{a} = 2.2 \cdot 10^{-12} \quad \mathrm{f(Hz)}. \tag{4}$$

This representation of the K-factor was found to be the simplest function to match the test data [5].

It is proposed that a digital filter matching this characteristic is used to process the measurement data and is either applied to the whole impulse waveform or just on the oscillations/overshoot (called residual data) [6]. Residual data are created by subtracting a mean curve from the raw data, where the mean curve has been fitted using a least mean squares approach. The mean curve is defined as a double exponential function, u(t), having four tunable parameters, such that

$$\mathrm{u(t)} = \alpha\left(\mathrm{e}^{-\frac{(\mathrm{t}-\mathrm{t_0})}{\tau_2}} - \mathrm{e}^{-\frac{(\mathrm{t}-\mathrm{t_0})}{\tau_1}}\right) \tag{5}$$

where α is a scalar (negative for negative impulses, positive for positive impulses) and τ_1 and τ_2 model the front and tail times, respectively. The filtered residual data are then added to the mean curve and the resulting waveform is used to determine the lightning impulse parameters. A comparison between both methods of applying the K-factor has been undertaken and reported [6], [7] and the residual filtering method is preferred to a global approach because it produces test voltage results that are consistent with empirical values obtained by experimentation. However, to apply the mean fitted curve properly, it is necessary to find the true origin $(\mathrm{t_0})$ of the raw measurement waveform [5]. The draft of the IEC 60060-1 revision proposes to define this point as the first instance that the raw data deviates from the measurement base by more than three standard deviations. The mean curve contains high-frequency components. Fig. 2 shows the spectrum for the worst-case acceptable mean curve that has a 0.84-μs front time, 40-μs tail time, and was zero-mean averaged before applying the Fourier transform to remove the 0-Hz component (i.e., the mean curve that will contain the largest proportion of high-frequency components). Filtering of residual data by subtracting a mean curve from the raw measurement data ensures that frequency components around 500 kHz that contribute to the impulse waveform are not attenuated by application of the

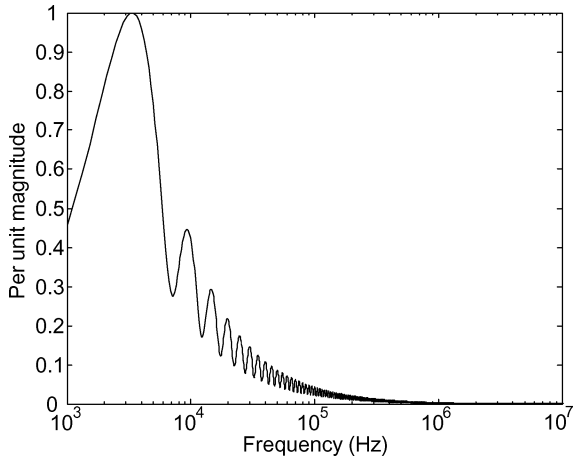

Fig. 2. Frequency spectrum of a mean curve representing an impulse waveform with 0.84-μs front time and 40-μs tail time.

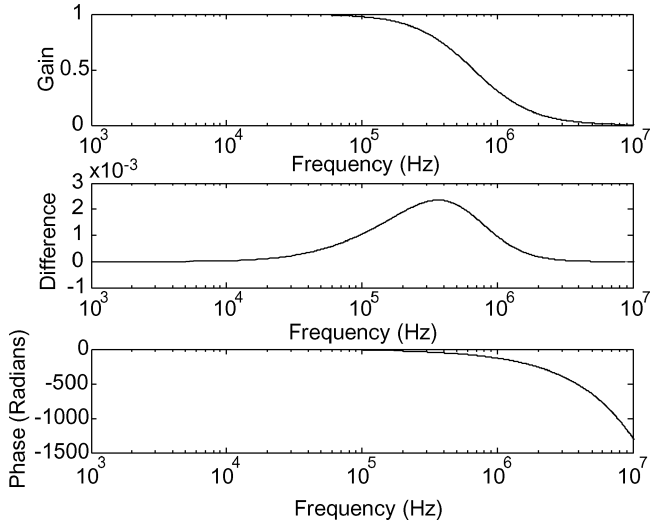

Fig. 3. Gain of an FIR filter of order 4096 designed to match $\mathrm{K_T}$, difference compared to $\mathrm{K_T}$ and filter phase response.

K-factor. Thus, compared to a global filtering approach, less information will be lost in the filtering process, providing a more representative curve for parameter estimation.

Studies have been undertaken in order to determine which digital filter best matches the K-factor characteristic [5]. Results have been presented for finite impulse response (FIR) and infinite impulse response (IIR) filter designs as well as methods using the fast Fourier transform (FFT) to appropriately scale the frequency components of the residual waveform. Filter designs have been produced independently and tested against a set of standard waveforms from IEC 61083-2. Results of these studies have shown that the FIR designs are a better match to the K-factor and their use produces less distortion to the impulse waveform than the IIR approach.

However, FIR designs are not without their disadvantages, as the filters are typically of very high order and they also introduce a linear phase lag. Fig. 3 shows the gain and phase of an FIR filter of order 4096 that has been designed to match the defined K-factor characteristic. It is worth noting that the FIR filter introduces a linear phase shift, which could influence parameter evaluation if the filter is not carefully constructed to ensure that the linear phase shift between the discrete frequency

components of the sampled input data is an integer number of 2π radians. The difference between the filter characteristic gain and the K-factor as a function of frequency is also shown. Over the range from zero to 500 kHz, the maximum difference is $2.4 \cdot 10^{-3}$ at 368 kHz, an error of less than 0.3%.

The ideal implementation of the K-factor characteristic would be in a form that has the advantages of having a low order as in IIR designs, is a good match to the K-factor as in FIR- and FFT-based design and does not introduce any additional phase shift as in IIR and FIR approaches. The following sections describe a method for achieving this and investigate the performance of the proposed design using the standard curves from the IEC 61083-2 test data generator and experimental impulse voltage waveforms generated at the Tony Davies High Voltage Laboratory, University of Southampton.

II. Zero-Phase Filtering

The main disadvantage of low-pass IIR filters is that they introduce phase lag across their passband. Causal filtering methods, where the current filter output is dependent on previous inputs/outputs, do not allow the removal of this additional nonlinear frequency-dependent phase shift. However, a noncausal implementation of a filter, where the current filter output is dependent on previous and future inputs/outputs, can result in filters that have a passband and stopband with zero phase shift. Due to the requirement to know the value of future inputs, this approach is only suitable for batch processing, where sets of measurement data do not need to be filtered online. The techniques of zero-phase filtering have found application in the control of repetitive processes [8] and are ideally suited to the batch filtering of impulse voltage waveforms.

The method used to create a zero-phase filter is to initially design a causal filter (for example, a lowpass Butterworth or FIR) that will act as a single stage of the implementation. A batch of data is filtered using the single stage and the resulting output is then reversed in order before being filtered again by the same single stage. After filtering for the second time, the output has to be reversed again so that the zero-phase filtered data are in the correct order. The reversing process between the two stages ensures that any phase lag added during the first stage is subtracted by the second stage. The double application of the single-stage filter to the data ensures a doubling of attenuation.

Generally, zero-phase filters are implemented around a single stage that has been designed using established techniques. For this application, it is possible to design a single stage using the K-factor defined in (4). The single stage must provide half of the attenuation of the K-factor.

A. Single-Stage Design

The first task is to define the single-stage filter characteristic based on the definition of $\mathrm{K_T}$. Expressing the magnitude of $\mathrm{K_T}$ in decibels and frequency in $\mathrm{rad \cdot s^{-1}}$ yields

$$|\mathrm{K_T}(\omega)| = -20\log_{10}\left(1+\frac{\mathrm{a}}{4\pi^2}\omega^2\right) \quad (\mathrm{dB}). \tag{6}$$

Therefore, the half magnitude can be expressed as

$$\frac{|\mathrm{K_T}(\omega)|}{2} = -10\log_{10}\left(1+\frac{\mathrm{a}}{4\pi^2}\omega^2\right) \quad (\mathrm{dB}). \tag{7}$$

This can be represented using a continuous function, G(s) defined as

$$\mathrm{G(s)} = \frac{1}{\frac{\mathrm{s}}{\omega_\mathrm{c}}+1} \tag{8}$$

where s is the Laplace operator and ω_c is the corner frequency $(\mathrm{rad \cdot s^{-1}})$. The filter magnitude at the corner frequency is defined as

$$\frac{|\mathrm{K_T}(\omega)|}{2} = -10\log_{10}(2) \quad (\mathrm{dB}). \tag{9}$$

Equating (7) and (9) defines the corner frequency as

$$\omega_\mathrm{c} = 2\pi\sqrt{\frac{1}{\mathrm{a}}} \quad (\mathrm{rad \cdot s^{-1}}). \tag{10}$$

The continuous function can be converted to discrete form using the bilinear transform, where the Laplace operator is mapped into discrete space using

$$\mathrm{s} \equiv \frac{2}{\mathrm{T}}\frac{\mathrm{z}-1}{\mathrm{z}+1} \tag{11}$$

where T is the sample interval (s). This approach will produce a digital filter whose frequency response (below the Nyquist frequency) is similar to the continuous function. However, it is also possible to "prewarp" the continuous function to ensure that the discrete form has an identical frequency response at a single defined frequency. In this case, the responses are matched at the corner frequency by replacing ω_c with Ω_c in (8), where Ω_c is defined as

$$\Omega_\mathrm{c} = \frac{2}{\mathrm{T}}\tan\left(\frac{\omega_c\mathrm{T}}{2}\right). \tag{12}$$

Applying (11) and (12) to (8) produces a discrete (prewarped) transfer function, G(z)

$$\mathrm{G(z)} = \frac{\frac{\tan\left(\frac{\omega_c\mathrm{T}}{2}\right)}{1+\tan\left(\frac{\omega_c\mathrm{T}}{2}\right)}(\mathrm{z}+1)}{\mathrm{z}-\frac{1-\tan\left(\frac{\omega_c\mathrm{T}}{2}\right)}{1+\tan\left(\frac{\omega_c\mathrm{T}}{2}\right)}}. \tag{13}$$

If the input to the single stage is defined as X(z) and its output as Y(z), then substituting for the corner frequency (10) and rearranging gives

$$\mathrm{G(z)} = \frac{\mathrm{Y(z)}}{\mathrm{X(z)}} = \frac{\frac{\tan\left(\frac{\pi\mathrm{T}}{\sqrt{\mathrm{a}}}\right)}{1+\tan\left(\frac{\pi\mathrm{T}}{\sqrt{\mathrm{a}}}\right)}(1+\mathrm{z}^{-1})}{1-\frac{1-\tan\left(\frac{\pi\mathrm{T}}{\sqrt{\mathrm{a}}}\right)}{1+\tan\left(\frac{\pi\mathrm{T}}{\sqrt{\mathrm{a}}}\right)}\mathrm{z}^{-1}}. \tag{14}$$

Equation (14) can be rewritten in the form of a difference equation such that the ith output of the single-stage filter, y(i) is

$$\mathrm{y(i)} = \frac{\tan\left(\frac{\pi\mathrm{T}}{\sqrt{\mathrm{a}}}\right)}{1+\tan\left(\frac{\pi\mathrm{T}}{\sqrt{\mathrm{a}}}\right)}(\mathrm{x(i)}+\mathrm{x(i-1)}) + \frac{1-\tan\left(\frac{\pi\mathrm{T}}{\sqrt{\mathrm{a}}}\right)}{1+\tan\left(\frac{\pi\mathrm{T}}{\sqrt{\mathrm{a}}}\right)}\mathrm{y(i-1)}. \tag{15}$$

Implementing this in a zero-phase format using a sampling period of 10 ns, gives a single-stage difference equation of

$$\mathrm{y(i)} = 0.02074433774260\,(\mathrm{x(i)}+\mathrm{x(i-1)}) + 0.95851132514810\mathrm{y(i-1)}. \tag{16}$$

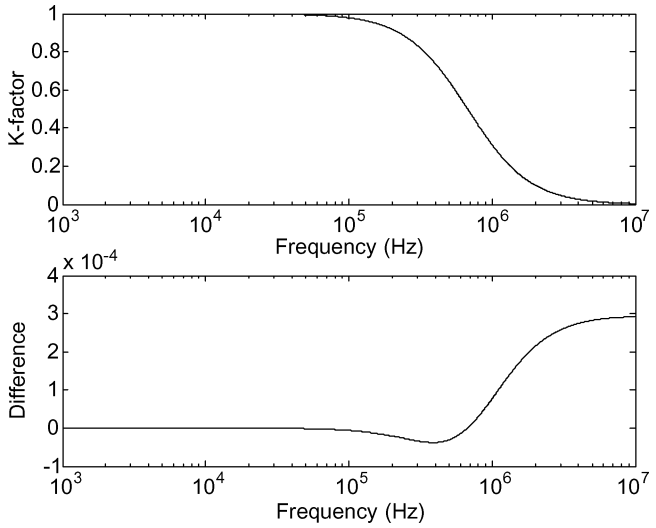

Fig. 4. Zero-phase filter (100 MS $\cdot s^{-1}$ sampling rate) frequency response and difference compared to K_T.

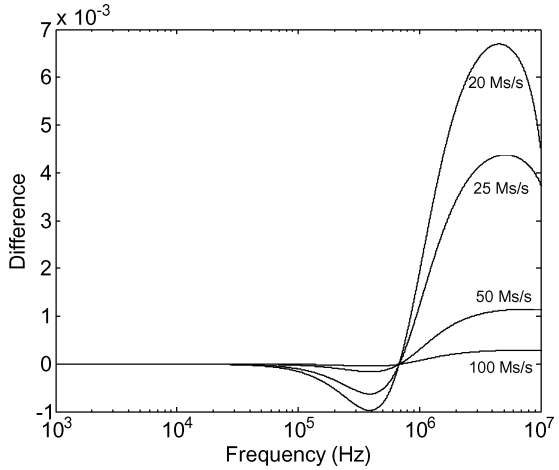

Fig. 5. Difference from K_T for zero-phase filters with sampling frequencies of 100 MS$\cdot s^{-1}$, 50 MS $\cdot s^{-1}$, 25 MS $\cdot s^{-1}$ and 20 MS $\cdot s^{-1}$.

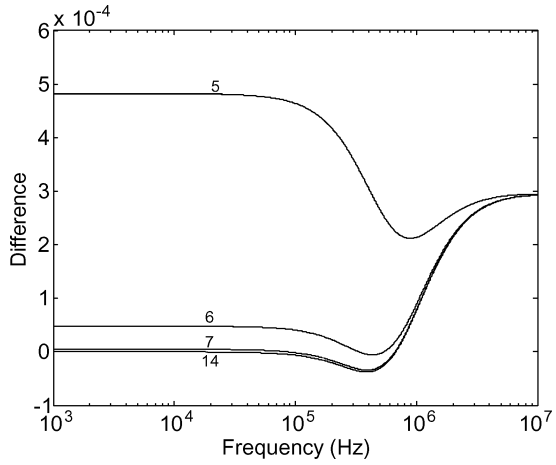

Fig. 6. Difference from K_T for the 100 MS$\cdot s^{-1}$ zero-phase filter for coefficient truncations of 14, 7, 6, and 5 places after the decimal point.

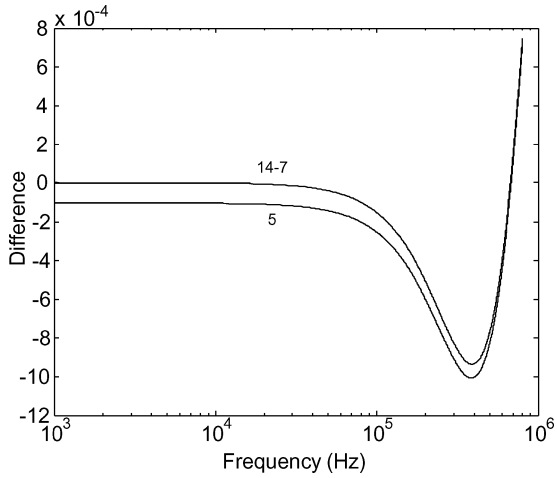

Fig. 7. Difference from K_T for the 20 MS$\cdot s^{-1}$ zero-phase filter for coefficient truncations of 14, 7, and 5 places after the decimal point.

The frequency response of the complete filter, implemented using coefficients with a precision of 14 places after the decimal point is shown in Fig. 4. The difference between the filter gain and the value of K_T across the frequency range is also shown. Over the range from zero to 500 kHz, the maximum difference in per unit gain is $3.7 \cdot 10^{-5}$ at 389 kHz, an error of less than 0.005%. This compares very favorably with the filter described in Fig. 3 and other reported higher order FIR filter designs [5], [8].

III. Practical Implementation

Considering the simplicity of the single-stage difference equation (15), there are two factors that will clearly influence the ability of the zero-phase filter to represent the K-factor, namely the choice of sampling frequency and the selected precision of the two coefficients. Fig. 5 shows the difference between K_T and the zero-phase filter implementation for four different sampling frequencies ranging from 100 $MS \cdot s^{-1}$ down to 20 $MS \cdot s^{-1}$. In all cases, the coefficients were implemented with a precision of 14 places after the decimal point. With reference to Fig. 5, all implementations perfectly match K_T at the single-stage corner frequency of 674 kHz and the largest difference from K_T below 500 kHz is always 389 kHz. In all cases, the zero-phase filter peak difference below 500 kHz is less than the 4096–order FIR filter designed with a sample period of 10 ns (Fig. 3).

The effect of truncating the single-stage coefficients has also been investigated and Fig. 6 shows the difference between the 100 MS$\cdot s^{-1}$ zero-phase filter and the K-factor as the precision of the single-stage coefficients are reduced from 14 places after the decimal point to 5 places. There is very little reduction in performance of the filter as the precision is reduced from 14 to seven places and, therefore, the corresponding plots are not included in Fig. 6. However, further reduction in precision has a significant effect on the overall match of the zero-phase filter with the K-factor. Similar results are achieved for designs with lower sampling rates although the errors are larger as the sampling rate is reduced. Fig. 7 shows the difference plots for the 20 MS$\cdot s^{-1}$ zero-phase filter and truncations of 14, 7, and 5 places after the decimal place over the frequency range of 1 to 800 kHz. The

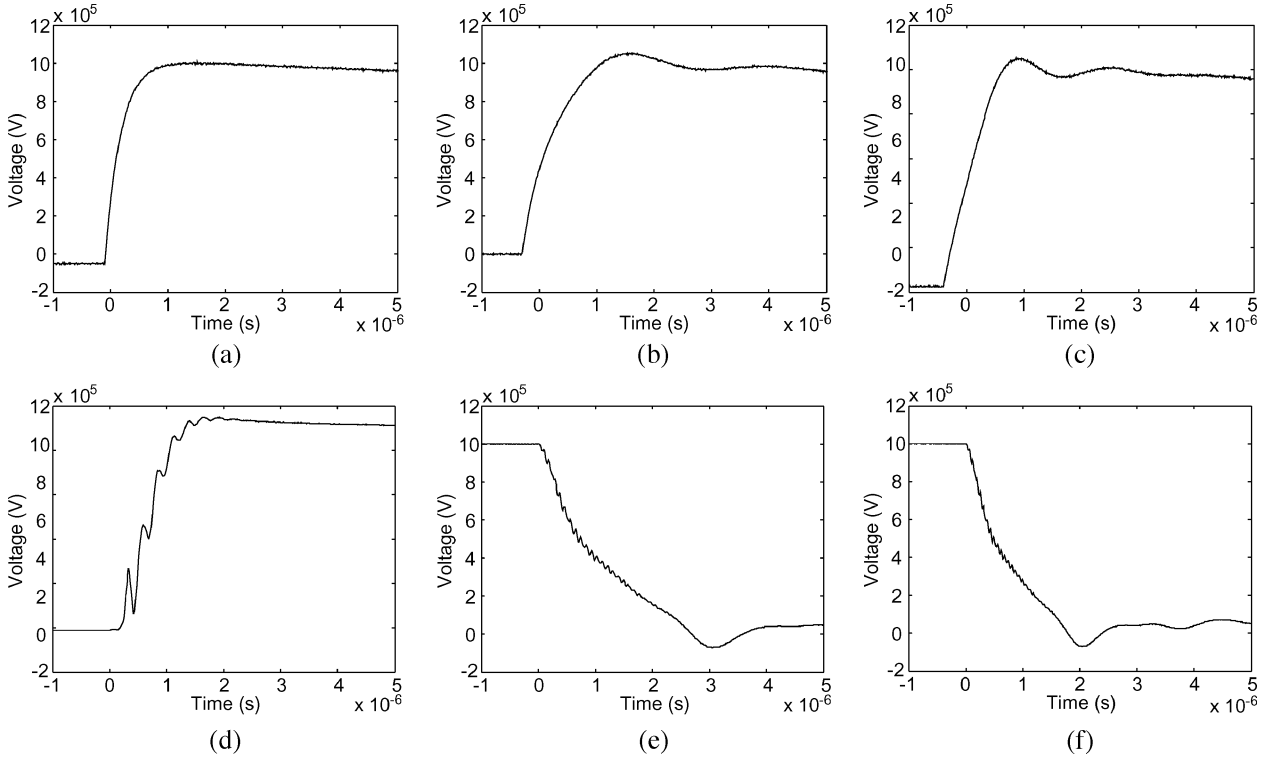

Fig. 8. IEC 601083-2 test data generator impulse waveforms. (a) Case 06. (b) Case 08. (c) Case 09. (d) Case 11. (e) Case 13. (f) Case 14.

difference plots are identical as the coefficient precision is reduced from 14 places to 7, and further reduction causes larger errors.

The results of this analysis indicate that a single stage designed using (15) should be implemented with a minimum coefficient precision of seven places after the decimal point. Ideally, the sampling frequency of the measurement system should be at least 20 $\mathrm{MS}\mathrm{s}^{-1}$ to ensure that the zero-phase filter is a good representation of the K-factor.

IV. Results

It has been established from other studies [5]–[7] that the residual filtering method is more appropriate than global filtering for parameter evaluation of the measured impulse waveform and, consequently, only the residual filtering approach has been implemented to assess the performance of the zero-phase K-factor filter. In all cases, the analysis uses a 100 $\mathrm{MS}\cdot\mathrm{s}^{-1}$ filter with a coefficient precision of 14 places after the decimal point.

A. IEC 601083-2 Test Data Generator Waveforms

Six impulse waveforms from the IEC test data generator have been analyzed using the zero-phase K-factor and an FIR filter of order 2048 designed to match the K-factor. The waveforms are shown in Fig. 8. Case 06 [Fig. 8(a)] is a double exponential waveform with noise, whereas cases 08 and 09 [Fig. 8(b) and (c)] also contain a long and short duration overshoot, respectively. Cases 11, 13, and 14 [Fig. 8(d)–(f)] are all measured waveforms, 13 and 14 contain long and short duration overshoots, respectively. Under the current standard, overshoots of less than 1 μs duration and noise or oscillations of frequency greater than 500 kHz can be ignored by using a mean curve to evaluate peak voltage, consequently the reference values supplied by the test data generator assume the complete removal of any overshoot. Table I shows the parameter values evaluated (front time, tail time, and peak voltage) using the two implementations of the K-factor (zero-phase and IIR filters) along with the reference values for the six impulse waveforms supplied from the IEC 601083-2 test data generator.

1) Peak Value Evaluation: Regardless of the chosen K-factor filter, only two of the obtained peak voltage values for the six test cases are within the reference values from the test data generator. This was as expected, since the change in the definitions will lead to different interpretations of the curves and to new reference values for the parameters.

For case 06 [Fig. 8(a)], there is no noticeable overshoot, the resulting curve obtained from the mean curve added to the filtered residual curve is almost identical to the original data and either implementation of K-factor is in agreement with supplied reference values.

Peak voltage and the time-to-half value for case 11 [Fig. 8(d)] are also in agreement with the reference value; however, the front time is not. In addition, the application of the K-factor to the residual waveform produces an overall waveform that has a negative voltage value around t_0. Fig. 9(a) shows the waveforms obtained when implementing the zero-phase K-factor on residual data for case 11.

The other four cases produce evaluations of peak voltage that are outside the range of test data generator reference values. In all of these cases, there is overshoot around the peak voltage. Fig. 9(b) shows the result obtained for applying the zero-phase K-factor to case 08 [Fig. 8(b)], the waveform for the parameter estimation contains an attenuated overshoot, leading to a

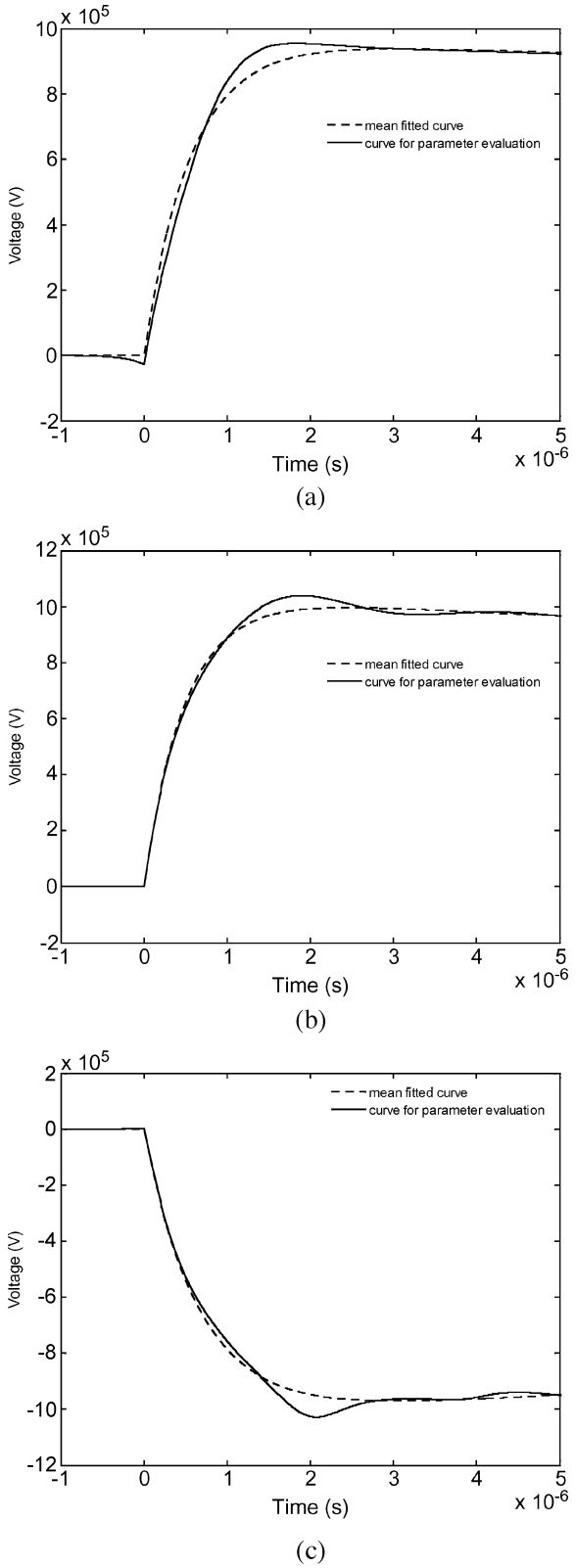

Fig. 9. Mean fitted curve and parameter evaluation curve (where residual data have been filtered using the zero-phase K-factor). (a) Case 11. (b) Case 08. (c) Case 14.

peak voltage parameter that is larger than the reference high value. The largest difference occurs for case 14 [Fig. 9(c)] as in this case inclusion of the attenuated short duration overshoot

TABLE I
COMPARISON OF EVALUATED PARAMETERS FOR IEC 61083 TEST DATA CURVES

IEC Case Number	Zero Phase K-factor	FIR filter K-factor	Reference Low	Reference High
	Peak Values (kV)			
06	1049.20	1049.23	1040.00	1060.00
08	1038.90	1038.76	1040.00	1060.00
09	998.05	998.43	960.00	990.00
11	954.61	954.89	940.00	960.00
13	-1043.20	-1042.80	-1060.00	-1080.00
14	-1027.90	-1027.67	-950.00	-970.00
	Front Times (μs)			
06	0.818	0.821	0.810	0.870
08	1.620	1.622	1.600	1.700
09	1.219	1.220	1.000	1.100
11	1.336	1.341	1.070	1.190
13	3.373	3.383	3.400	3.760
14	2.154	2.178	1.850	2.050
	Tail Times (μs)			
06	60.166	60.159	57.50	62.50
08	47.473	47.484	45.00	49.00
09	48.341	48.323	48.00	52.00
11	87.426	87.389	82.00	91.00
13	61.437	61.480	56.00	62.00
14	41.891	41.894	43.00	47.00

when calculating the peak voltage leads to a parameter that is 6% higher than the test data generator high reference value. Under the current standard, it is acceptable to measure the peak voltage from the mean curve and, in this case, it would result in a significantly lower peak voltage.

2) Front-Time Evaluation: A comparison of the obtained front times detailed in Table I shows that the values obtained for cases 06 and 08 are within the reference limits whereas the application of the K-factor for cases 09, 11, and 14 results in front-time parameters in excess of their respective high reference value. For case 13, the obtained front time is slightly lower than the reference low value. The largest discrepancy is for case 11, which has oscillations on the rising edge [Fig. 8(d)]. With reference to Fig. 9(a), the addition of the K-filtered residual to mean increases the front time to a value that is 13% above the reference high value.

3) Tail Time Evaluation: The results obtained for tail times are within the reference values supplied by the test data generator, with the exception of case 14 [Fig. 9(c)]. In this case, the K-factor increases the peak voltage parameter and this effectively reduces the t_{50} because the U_{50} value is greater.

4) Zero-Phase Filter Performance: Comparing the relative performance of the IIR filter against that of the FIR implementation across the six test cases reveals that both implementa-

TABLE II
COMPARISON OF EVALUATED PARAMETERS FOR LABORATORY-GENERATED IMPULSE WAVEFORMS

Experiment Number	Zero Phase K-factor	FIR filter K-factor	IEC60060-1 mean curve by least squares regression (mean curve by eye)
	Peak Values (kV)		
01	100.11	100.13	100.06
02	-149.28	-149.31	-149.84
03	104.96	105.07	103.95 (101.08)
	Front Times (μs)		
01	1.353	1.344	1.253
02	1.369	1.380	1.253
03	0.618	0.616	0.752 (0.384)
	Tail Times (μs)		
01	45.840	45.831	44.866
02	45.800	45.790	43.399
03	38.461	38.421	38.997 (39.001)

tions yield similar values for evaluated parameters (Table I). The largest discrepancy in peak voltage estimation occurs in case 13 and is 400 V. In the results for the rise time, the largest difference is 28 ns for case 14 and for the tail time, case 13 has a difference of 43 ns. There are two reasons for these differences: first, as shown in Figs. 3 and 4, the zero-phase filter implementation is a closer match to the defined K-factor and second, the comparative low order of the zero-phase filter ensures that any computational errors (e.g., roundup errors) are minimal.

B. Application to Measured Impulse Voltage Waveforms

Three impulse waveforms generated experimentally have also been analyzed using the zero-phase filter design and the obtained results are shown in Table II. In Table II, experiments 1–3 correspond to Fig. 10(a)–(c), respectively. The voltage waveforms have been generated using a two-stage Marx generator, a Haefely–Trench Multitest HV-KIT. The measurement of impulse waveforms is performed using a capacitor divider; an output from the capacitor divider has been captured using a Tektronix TDS 520C digital storage oscilloscope (DSO) and scope probe for $\times 10$ attenuation. The high-voltage capacitor divider is an approved and calibrated measuring device in accordance with IEC 60060-2 and-3. The DSO is calibrated and traceable to national standards and the scope probe compensated in accordance with the guidance of IEC 60060-2.

Fig. 10(a)–(c) is unprocessed waveforms which have been generated from the two-stage Marx generator with no load in circuit. All three waveforms display noise near the origin, but this is permissible as specified by IEC 60060-1, because it does not occur on the part of the waveform in excess of 90% of the peak voltage. The noise is due to electromagnetic coupling from the test generator to the DSO input and was deliberately

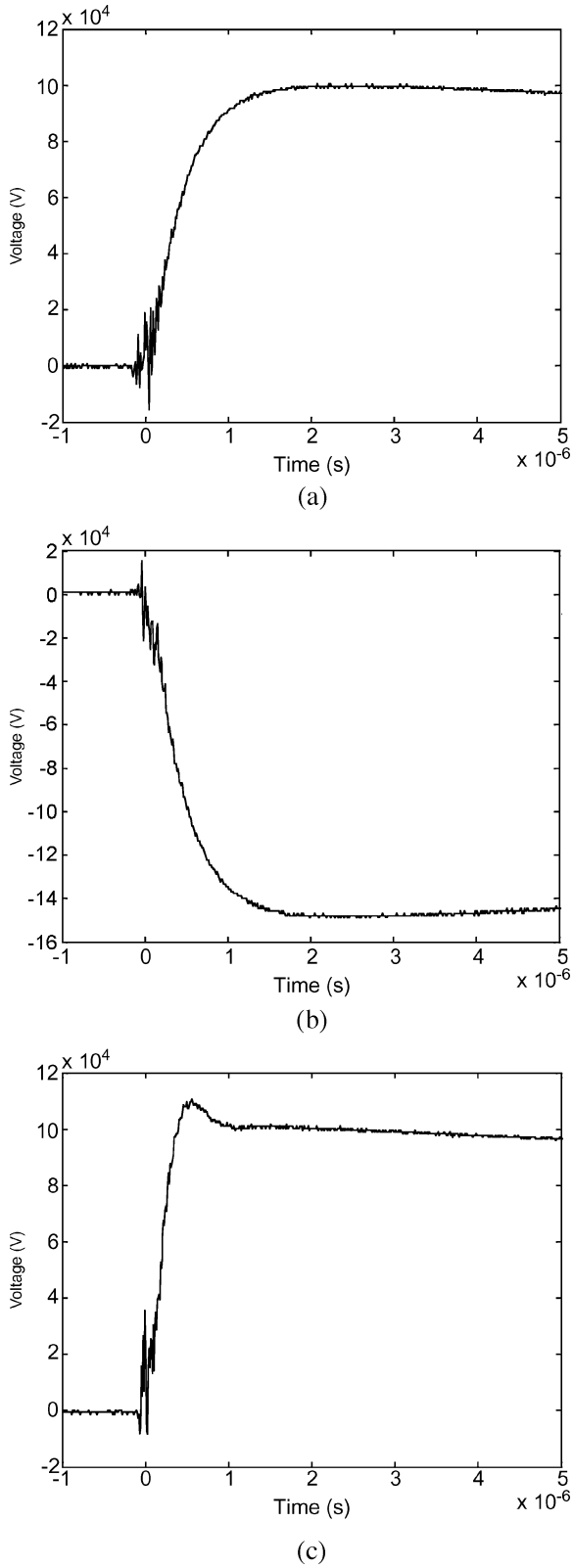

Fig. 10. Experimentally generated impulse voltages.

permitted in order to experimentally evaluate the performance of the proposed digital filtering techniques. Fig. 10(a) and (b) are full-lightning impulse waveforms, positive and negative impulses, respectively, and the zero-phase K-factor and a mean curve are shown in Figs. 11(a) and (b), respectively.

3. Peak Value Evaluation

The peak values obtained for experiment 1 and 2 using the zero-phase and FIR K-factor are close to that obtained from the raw data. Fig. 10(c) has a faster front time and overshoot, this has been achieved by reducing the wavefront control resistors of the Marx generator circuit, the resulting front time is faster than permissible by the current standard when parameters are evaluated using any of the three techniques investigated. However, this waveform illustrates the following points of interest. Using the IEC 60060-1 standard, the overshoot at the peak of the wave has a duration of less than 1 μs and, thus, is to be discounted by drawing a mean curve. The interpretation of a suitable method to fit a mean curve is left to the operator. This may have traditionally been performed by eye. By being performed in this way, a curve has been drawn providing the peak value in Table II of 101.8 kV, some 3.8% lower than the largest value found using the FIR filter, and 2.8% lower than using a double exponential mean curve (5) plotted using an LMS method. The selection of peak is significant as it influences the results for virtual origin and front time found using (1) and (2); and tail time which is also dependent on the obtained virtual origin (3).

1) Front-Time Evaluation: Front times found by IEC 60060-1 [i.e., from the raw data and using (1)] are the same for experiments 1 and 2 [Fig. 10(a) and (b)] as is to be expected, the circuit including the front-time resistors for these two experiments is identical. The variation in the front times between the IEC 60060-1 result and the K-factor results is due to the initial noise causing the waveform to rise from the baseline earlier when filtered and an earlier virtual origin being defined. The virtual origin is sensitive to the gradient of the line plotted through the 30% and 90% voltage points. The additional time difference between IEC 60060-1 and K-factor front times is also seen in the difference between results for tail times.

2) Tail Time Evaluation: In addition to the raw data, Fig. 11(c) shows a mean curve plotted by the use of an LMS method and the evaluation curve filtered using the new zero-phase filter for the K-factor. A curve fitted by a human operator can remove the overshoot completely and has no offset error on the waveform tail, thus the peak is estimated to be lower than either the computed mean curve or zero-phase K-factor curve which both display some overshoot. The disadvantage of fitting a mean curve by eye is that it is less objective in application than using a defined digital technique. With reference to Fig. 11(c), the computed mean curve from the raw data moderately smoothes the overshoot, but results in a detrimental offset error between the mean curve tail and the original measurement tail; whereas the addition of the residual, filtered using the zero-phase K-factor, reduces the influence of the overshoot and matches the tail of the original measurement precisely.

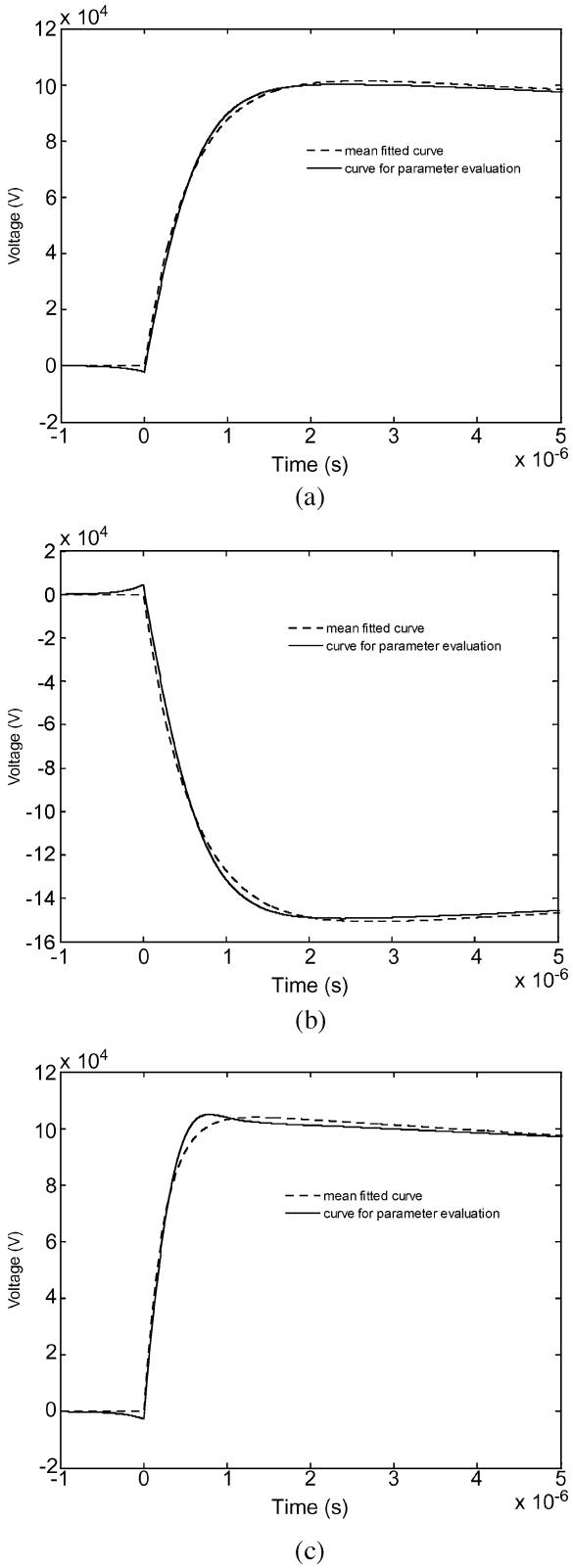

Fig. 11. Experimental results of the mean fitted curve and parameter evaluation curve (where residual data have been filtered using the zero-phase K-factor). (a)–(c) correspond to raw data plots in Fig. 10.

V. Discussion

Proposed changes to IEC60060-1 include the use of a residual filtering method before measurement of the impulse waveform

parameters. To apply the method, it is necessary to fit a double exponential curve (5) which has a true origin t_0, defined as the first instance that the raw measurement deviates from the base line by more than three standard deviations. Having obtained a mean curve, this is subtracted from the measurement data to produce a residual. The residual is filtered using a filter designed to match the predefined K-factor (4) and the result added to the mean curve. This curve is then used to evaluate the three impulse parameters, namely: peak voltage, front time, and tail time to 50% of peak, using the same methodology as in the current standard.

Parameter results obtained for six cases from the IEC 601083-2 test data generator show that this approach yields peak voltages that are higher than those obtained using the current standard if there are oscillations or overshoot around the peak voltage. This is a considerable change from the existing approach because these effects are now taken into account, whereas currently it is assumed that overshoots and oscillations have a minimal effect on the test object. Under the existing standard, it is acceptable to use a mean curve to determine the peak voltage, consequently underestimating the true value that may be seen by the test object. However, it would appear that the residual method also effects the front-time measurement, especially in cases where there are oscillations on the rising edge of the waveform. This, in part, may be due to the method of defining the true origin as the first time that the measurement deviates from the base value by more than three standard deviations. Laboratory-generated impulse waveforms with significant noise at the start of the rising edge demonstrate that the three standard deviation definition of the true origin will cause t_0 to be defined earlier than the value obtained using (2), thus increasing the value of the front time. The tail times are less sensitive and are not greatly affected by the application of the three standard deviation method.

It is important that having subtracted a well-fitted mean curve from the raw measurement data, any operations on the residual data do not introduce phase shift, as this may, in turn, affect the parameter values. The obtained results in Tables I and II demonstrate that different parameter values are obtained depending on how the K-factor is implemented. The two implemented filters (designed to ensure zero-phase shift) were used on the same residual data and the small differences in values of obtained parameters must be due to the difference of closeness with which the filters match the characteristic of the defined K-factor.

The additional complexity of implementing a noncausal filter to process a batch of residual data should be considered in the context of fitting a mean curve to the raw data having established the true origin of the waveform. The requirement to apply a low-order filter twice, reversing the data order after each application is trivial in comparison.

VI. Conclusion

Implementing the K-factor using a zero-phase filter, having a single stage described by (15) has advantages over other proposed approaches: Overall, the filter is only second order, it does not influence the phase of the residual data and results from tests show that it performs as well if not better than FIR filters of orders up to 4096. Another advantage is that the coefficients can be easily calculated using simple formulae. This allows the analysis software to quickly determine new filter coefficients when the sampling frequency is changed. In August 2007, IEC TC42 agreed to propose this zero-phase filter for the next revision of IEC 60060-1 as the preferred way to perform K-factor filtering.

Results from the adoption of the proposed K-factor filtering method show that the peak value is found to be greater than the current mean-curve fit. This is a result of now taking account of the residual, a filtered output of oscillations and overshoot. Inspection of the front times has highlighted a potential difficulty with defining the virtual origin as the point where the voltage rises three standard deviations from the baseline, which is seen to be highly sensitive to signal noise at the start of the waveshape. Methods to best overcome this challenge will be the subject of a further paper.

References

[1] IEC 60060-1:1989, "High voltage test techniques"—Part 1 "General definitions and test requirement" Int. Electrotech. Comm..

[2] J. Rungis and Y. Li, "Precision digital filters for high voltage impulse measurement systems," *IEEE Trans. Power Del.*, vol. 14, no. 4, pp. 1213–1220, Oct. 1999.

[3] K. Hackemack, P. Werle, E. Gockenbach, and H. Borsi, "A new proposal for the evaluation of lightning impulses," in *Proc. 6th Int. Conf. Properties Applications Dielectric Materials*, Xi'an, China, Jun. 21–26, 2000, pp. 93–96.

[4] P. Simon, F. Garnacho, Berlijn, and E. Gockenbach, "Determining the test voltage factor function for the evaluation of lightning impulses with oscillations and/or an overshoot," *IEEE Trans. Power Del.*, vol. 21, no. 2, pp. 560–566, Apr. 2006.

[5] J. Hällström, S. Berlijn, M. Gamlin, F. Garnacho, E. Gockenbach, T. Kato, Y. Li, and J. Rungis, "Applicability of different implementations of K-factor filtering schemes for the revision of IEC60060-1 and -2," presented at the 14th Int. Symp. High Voltage Engineering, Beijing, China, August 25–29, 2005, B-3.

[6] Y. Li and J. Rungis, "Evaluation of parameters of lightning impulses with overshoot," presented at the 13th Int. Symp. High Voltage Engineering, Delft, The Netherlands, Aug. 25–29, 2003.

[7] M. Gamlin, "Implementation of the K-factor for the lightning impulse evaluation by means of digital FIR filtering," presented at the 14th Int. Symp. High Voltage Engineering, Beijing, China, Aug. 25–29, 2005, B-79.

[8] R. W. Longman, "Iterative learning control and repetitive control for engineering practice," *Int. J. Contr.*, vol. 73, no. 10, pp. 930–954, 2000.

Paul L. Lewin (M'05) was born in Ilford, U.K., in 1964. He received the B.Sc. (Hons.) and Ph.D. degrees in electrical engineering from the University of Southampton, Southampton, U.K., in 1986 and 1994, respectively.

He joined the academic staff of the University of Southampton in 1989, where he is currently a Reader of electrical power engineering in the School of Electronics and Computer Science. His research interests include condition monitoring of high-voltage (HV) cables and plant, surface charge measurement, HV insulation/dielectric materials, and applied signal processing. Since 1996, he has published many refereed conference and journal papers in these research areas. He is the Manager of the Tony Davies High Voltage Laboratory at the University of Southampton

Dr. Lewin is a chartered engineer and a member of the Institution of Electrical Engineers. He was the General Chair of the IEEE International Conference on Solid Dielectrics 2007 held in Winchester, U.K.

Trung N. Tran was born in Hanoi, Vietnam, in 1984. He received the B.Eng. degree from the University of Southampton, Southampton, U.K., under the sponsorship of the Electricity of Vietnam in 2006. He is currently pursuing the Ph.D. degree at the Tony Davies High Voltage Laboratory at the University of Southampton.

David J. Swaffield (M'05) was born in Epsom, U.K., in 1977. He received the Master's degree in electromechanical engineering and the Ph.D. degree from the School of Electronics and Computer Science at the University of Southampton, Southampton, U.K., in 2000 and 2005, respectively.

He joined the academic staff of the University of Southampton in 2007. His research interests include cryogenic dielectrics for superconducting apparatus, FEA modeling for electrical engineering applications, and high-voltage testing techniques.

Dr. Swaffield received the 2005 Eric Foster Young Scientist Award for a paper titled "Partial discharge characterization in liquid nitrogen composite systems" presented at ICDL2005.

Jari K. Hällström was born in Lappeenranta, Finland, in 1961. He received the M.Sc. and D.Sc. degrees in electrical engineering from the Helsinki University of Technology, Espoo, Finland, in 1987 and 2002, respectively.

Since 1984, he has held various positions at the Helsinki University of Technology. His first research interest was instrumentation for the measurement of magnetic fields of the human brain, and since 1994, high-voltage metrology. Since 2004, he has been responsible for the Finnish National Standards for high-voltage measurements.

Dr. Hällström was awarded the IEC 1906 Award for his work on standardization of high-voltage measuring techniques in 2007.